

Climate changes in temperature and precipitation extremes in an alpine grassland of Central Asia

Zengyun Hu¹ · Qingxiang Li² · Xi Chen¹ · Zhidong Teng³ · Changchun Chen⁴ · Gang Yin^{1,5} · Yuqing Zhang⁴

Received: 21 February 2015 / Accepted: 15 July 2015 / Published online: 13 August 2015
© Springer-Verlag Wien 2015

Abstract The natural ecosystem in Central Asia is sensitive and vulnerable to the arid and semiarid climate variations, especially the climate extreme events. However, the climate extreme events in this area are still unclear. Therefore, this study analyzed the climate variability in the temperature and precipitation extreme events in an alpine grassland (Bayanbuluk) of Central Asia based on the daily minimum temperature, daily maximum temperature, and daily precipitation from 1958 to 2012. Statistically significant ($p < 0.01$) increasing trends were found in the minimum temperature, maximum temperature at annual, and seasonal time scales except the winter maximum temperature. In the seasonal changes, the winter temperature had the largest contribution to the annual warming. Further, there appeared increasing trends for the warm nights and the warm days and decreasing trends for the cool nights and the cool days at a 99 % confidence level. These trends directly resulted in an increasing trend for the growing season length (GSL) which could have positively influence on the vegetation productivity. For the precipitation, it displayed an increasing trend for the annual

precipitation although it was not significant. And the summer precipitation had the same variations as the annual precipitation which indicated that the precipitation in summer made the biggest contribution to the annual precipitation than the other three seasons. The winter precipitation had a significant increasing trend (1.49 mm/10a) and a decreasing trend was found in spring. We also found that the precipitation of the very wet days mainly contributes to the annual precipitation with the trend of 4.5 mm/10a. The maximum 1-day precipitation and the heavy precipitation days only had slight increasing trend. A sharp decreasing trend was found before the early 1980s, and then becoming increase for the above three precipitation indexes. The climate experienced a warm-wet abrupt climate change in the 1980s. Further, this tendency may be continuous into the future.

1 Introduction

Climate change is a change in the climate state that can be identified (e.g., by using statistical tests) by changes in the mean and/or the variability of its properties and that persists for an extended period (IPCC 2012). And it is generally accepted that changes in the frequency or intensity of extreme weather and climate events would have more great impacts on both human society and natural systems than the mean climate variables (Easterling et al. 2000a, b; Patz et al. 2005; McMichael et al. 2006; IPCC 2012; Thornton et al. 2014).

In recent years, a number of weather events cause large losses of life and a tremendous increase in economic losses (Easterling et al. 2000a) all over the world, such as Hurricane Andrew in South Florida in 1992 (Changnon et al. 2000), the major floods in China in 1998 (The Ministry of Water Resources of the People's Republic of China's 1999). These evidences indicate that the study of the extreme climate events

✉ Xi Chen
chenxi@ms.xjb.ac.cn

¹ State Key Laboratory of Desert and Oasis Ecology, Xinjiang Institute of Ecology and Geography, Chinese Academy of Sciences, Urumqi 830011, China

² National Meteorological Information Center, China Meteorological Administration, Beijing, China

³ College of Mathematics and System Sciences, Xinjiang University, Urumqi 830046, China

⁴ School of Atmospheric Science, Nanjing University of Information Science and Technology, Nanjing, China

⁵ University of Chinese Academy of Sciences, Beijing, China

is urgent and important from which we can obtain useful information for managing the risks of extreme events and disasters.

Therefore, more and more attentions have been focused on the extreme changes of the temperature and precipitation at the global and regional scales (Janowiak 1990; Katz and Brown 1992; Frich et al. 2002; Zhai et al. 2005; Sun et al. 2014). Since the start of the twentieth century, the 0.6 °C increase of the global mean temperature (IPCC 1995) is associated with a stronger warming in daily minimum temperature than in maximums leading to a decrease in the diurnal temperature range (DTR) (Karl et al. 1993). From 1950 to 1993, the increasing trend for the minimum temperature is 1.86 °C/100a bigger than the 0.88 °C/100a trend for the maximum temperature overall global (Easterling et al. 1997). During 1951–2003, over 70 % of the land area sampled experienced a significant increase for the warm nights and a significant decrease for the cold nights (Alexander et al. 2006). But the precipitation changes are much less spatially coherent compared with temperature change (Alexander et al. 2006; IPCC 2013). A tendency toward wetter conditions is found over a large region of the Northern Hemisphere midlatitudes (Alexander et al. 2006) and a reduction is found in low latitude (IPCC 2013). Zhai et al. (2005) pointed that the extreme precipitation typically accounts for 30–40 % of annual precipitation over the whole China during 1951–200, although it is little trend in total precipitation in this period. In addition, significant increases in extreme precipitation were found in western China. In Central America and northern South America, there exists a significant increasing trend for the precipitation intensity. In addition to the observational studies, the climate models are applied to investigate the climate extremes, although there are still some systematic errors and limitations in accurately simulating regional climate conditions (Easterling et al. 2000a; Kharin et al. 2007; Chen et al. 2014; Pei et al. 2014). Sillmann et al. (2013a) displayed that the CMIP5 models have the ability to simulate climate extremes and their trend patterns for the present climate.

Central Asia is located at the hinterland of the Eurasian continent and far from the sea. On the other hand, the basins in the area are in the rain shadows of high mountain ranges. Adding its complex topography, this region has an arid and semiarid climate. Consequently, the ecosystems in Central Asia are sensitive and vulnerable to the climate change, such as the evapotranspiration, temperature, and precipitation, especially to the extreme climate events (Chen et al. 2012; Hu et al. 2013; Zhang et al. 2013; Hu et al. 2014; Dai et al. 2015). Bayanbuluk grassland has a special alpine mountain climate in Central Asia and is surrounded by snow-capped mountains (Hu et al. 2004). This grassland is also the largest alpine grassland in Xinjiang, China, and plays a key role on the local livestock development. Then, the climate study (especially the extreme climatic events) of the Bayanbuluk grassland

could provide great important information for the society and natural systems.

The objective of this paper is to provide a comprehensive analysis of observed temperature and precipitation (including the extreme climate events) in the Bayanbuluk grassland during the period of 1958–2012. Firstly, the results of analyses on the trends and variability of the climate will be presented, including both the annual and seasonal means. Secondly, for detecting the climate transformation in this study period, the abrupt climate change is discussed by the nonparametric Mann-Kendall method. And the long-rang dependence (LRD) of the climate is also investigated by the Hurst index. Thirdly, the extremes climate events will be analyzed, including the variability, abrupt climate change, and LRD. Finally, the comprehensive discussion and conclusion are provided.

2 Study area, data and methodologies

2.1 Study area and data

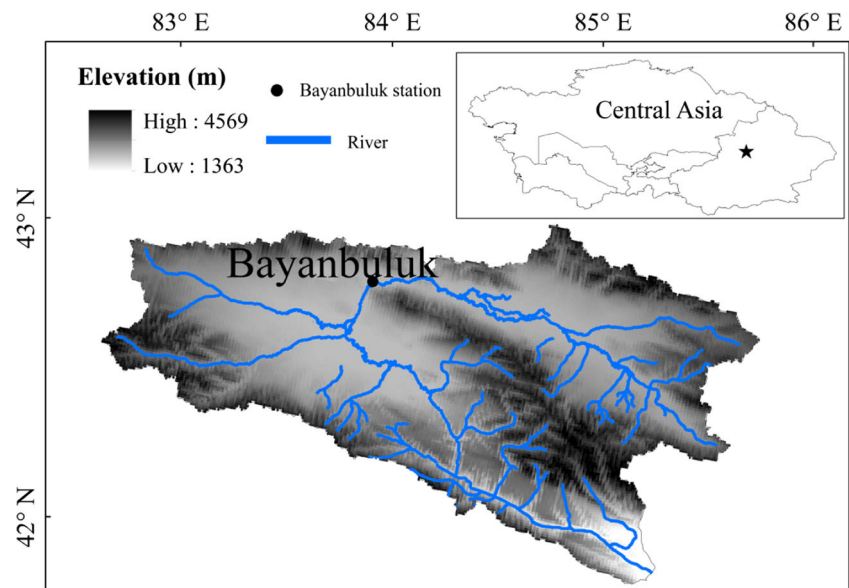
The Bayanbuluk grassland lies into the mountain basin of the central Tianshan Mountainous and the northwest of the Hejing country in Xinjiang Uygur Autonomous Region (Fig. 1). As the biggest alpine grassland in China, it covers more than 2.38×10^4 km² with the elevation from approximately 1400 to 4500 m. Affected by its topography, the Bayanbuluk grassland has a special alpine mountain climate: the annual mean temperature is −4.5 °C, the growing season (April–September) temperature is approximately between 5 and 10 °C, and the multi-annual mean precipitation is 270 mm (Hu et al. 2004).

In this study, the climate data daily T_{\max} , T_{\min} , and precipitation are from the National Meteorological Information Center (NMIC) of China Meteorological Administration (<http://www.cma.gov.cn/2011qx/fw/2011qs/jgx/>) during the period of 1958–2012. All the data are processed strictly, quality controlled, and homogeneity adjusted (Xu et al. 2013). The daily mean temperature (T_{mean}) is averaged from the daily T_{\max} and T_{\min} . For detecting the temperature variability, the diurnal temperature range (DTR) is calculated from the T_{\max} and T_{\min} . The seasonal and annual data are computed based on the daily data. The four seasons are spring [March, April, and May (MAM)], summer [June, July, and August (JJA)], fall [September, October, and November (SON)], and winter [December, January, and February (DJF)].

2.2 Methodologies

The trends of the temperature and precipitation are computed by the linear least square method at seasonal and annual time scales, respectively. And the statistically significance of the trend is tested by the *t* test method. As well known, the

Fig. 1 Topography and river network in Bayanbuluk area. The star means the study area in Central Asia



nonlinearity of the climate system may lead to abrupt climate change which means the state of the climate system transformed from one to another (Alley et al. 2003; IPCC 2012). The nonparametric Mann-Kendall method established by Mann (1945) and Kendall (1948) can not only detect the abrupt climate change but also obtain the trend of the time series (Fraedrich et al. 1997; Burn et al. 2002; Sayemuzzaman et al. 2015). Further, the Mann-Kendall method has no assumption on the distribution of the time series and is robust to the effect of outliers. The detailed information of the Mann-Kendall method can be found in Li et al. (2011).

The LRD (also referred to as long-term persistence, long memory, or Hurst phenomenon) and self-similar processes denote the property of time series to exhibit persistent behavior (Samorodnitsky 2006; Koutsoyiannis and Montanari 2007; Rea et al. 2011). LRD indicates the process is compatible with the presence of fluctuations on a range of timescales which can reflect the long-term variability of the time series, and it can be

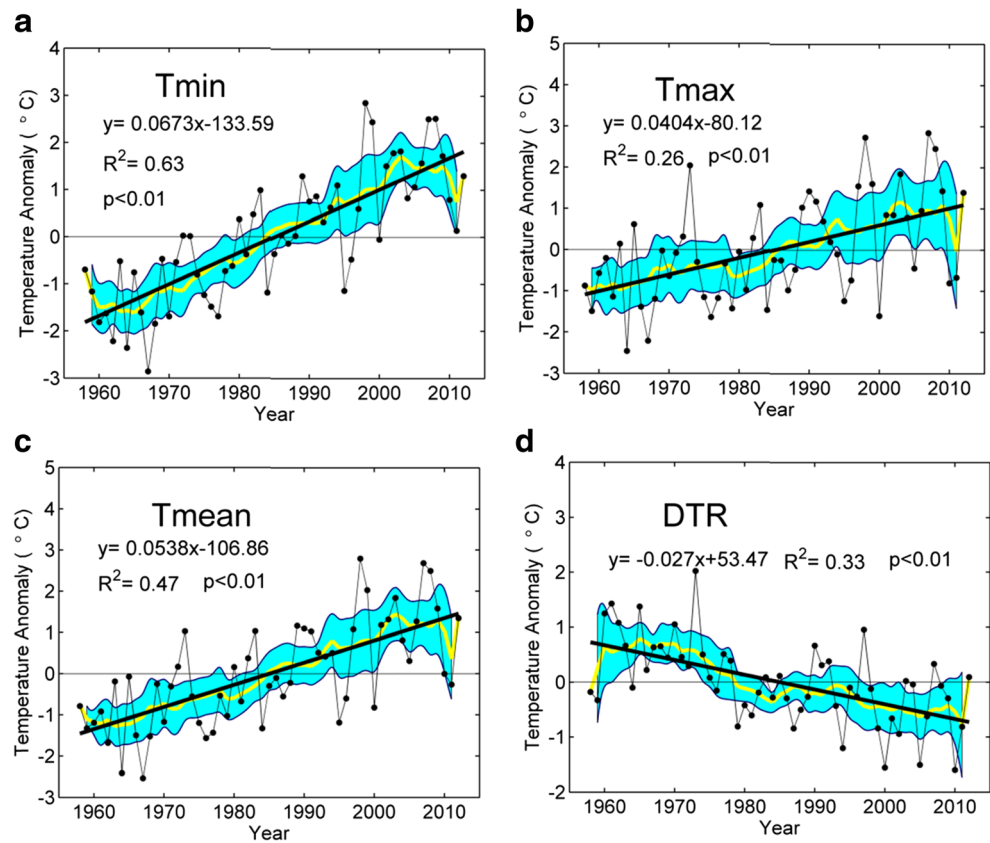
also defined as a tendency of clustering in time of similar events (droughts, floods, etc. Koutsoyiannis and Montanari 2007). A number of past studies (Bloomfield and Nychka 1992; Rybski et al. 2006; Zhu et al. 2010; Mann 2011; Rea et al. 2011) have investigated the variation of the LRD in climate records.

The Hurst index (H) is widely used to estimate the LRD of the time series in climate change, hydrology, and other fields (Koutsoyiannis 2003; Sakalauskiene 2003; Koutsoyiannis and Montanari 2007; Rehman 2009; Rehman and Siddiqi 2009; Velasquez Valle et al. 2013). According to the H value, the time series is classified in three cases: (1) $H = 0.5$ means the various essential elements is completely independent, and the time series is random; (2) $0.5 < H \leq 1$ indicates that the time series has a LRD which means persistent, and the bigger value, the stronger the continuity; and (3) $0 < H < 0.5$ also means the LRD which means anti-persistent, and the closer the H value to 0 indicates the stronger reverse tendency in future.

Table 1 Precipitation and Temperature Indices with their Definitions and Units

ID	Indicator name	Definitions	Units
GSL	Growing season Length	Annual (1st Jan. to 31st Dec. in NH, 1st July to 30th June in SH) count between first span of at least 6 days with $TG > 5^\circ\text{C}$ and first span after July 1 (January 1 in SH) of 6 days with $TG < 5^\circ\text{C}$	Days
TN10p	Cool nights	Days with $T_{\min} < 10\text{th}$ percentile of the same day during the base period 1961–1990	Days
TX10p	Cool days	Days with $T_{\max} < 10\text{th}$ percentile of the same day during the base period 1961–1990	Days
TN90p	Warm nights	Days with $T_{\min} > 90\text{th}$ percentile of the same day during the base period 1961–1990	Days
TX90p	Warm days	Days with $T_{\max} > 90\text{th}$ percentile of the same day during the base period 1961–1990	Days
RX1day	Max 1-day precipitation amount	Monthly maximum 1-day precipitation	mm
R10	Number of heavy precipitation days	Annual count of days when $\text{PRCP} \geq 10$ mm	Days
CDD	Consecutive dry days	Maximum number of consecutive days with $\text{RR} < 1$ mm	Days
R95pTOT	Very wet days	Annual total PRCP when $\text{RR} > 95\text{th}$ percentile of the same day during the base period 1961–1990	mm

Fig. 2 The temperature anomalies trends for annual mean T_{\min} (a), T_{\max} (b), T_{mean} (c), and DTR (d) during 1958–2012, respectively. The *thick black line* is the linear fit result calculated by the linear least square method. The *yellow curve* is the 11-year moving average. The *cyan color area* is the 95 % confidence interval envelope



As an important part of fractal theory, the rescaled range analysis (R/S , for a real-valued time series $\{x_1, x_2, \dots, x_n, \dots\}$, $S(n)$ is the standard deviation of the first n data of the series $\{x_1, x_2, \dots, x_n\}$ and R is their range: $R(n) = \max\{x_1, x_2, \dots, x_n\} - \min\{x_1, x_2, \dots, x_n\}$) method created by Hurst (1951) is the most classical method to compute the H parameter (Sanchez et al. 2008). In this paper, the R/S method is used to compute the H value.

For analyzing the extreme climate changes, we select 9 indices (5 for the temperature, 4 for the precipitation) from the 27 climate extremes indices of Expert Team on Climate Change Detection and Indices [(ETCCDI) <http://www.climdex.org/indexes.html>, Karl and Nicholls 1999; Peterson et al. 2001; Zhang et al. 2005] to detect the frequency and intensity of the climate change (Table 1). And these indices are computed by the RClimDex software. The change trends

of the 9 climate extremes indices are obtained by the linear least square method. The relationships between the climate extremes indices and the annual precipitation are quantified by the two-tailed Pearson correlation coefficients (CC). Moreover, the abrupt climate change and the long-term memory of the climate extreme indices are also detected by the Mann-Kendall method and the Hurst index, respectively.

3 Results

3.1 Trends in temperature and precipitation

Figure 2 shows the significant warming trends ($p < 0.01$) of the annual temperature indices during 1958–2012. The annual T_{\min} has the biggest increasing trend ($0.67 \text{ } ^\circ\text{C}/10\text{a}$). The

Table 2 The linear trend ($^\circ\text{C}/10\text{a}$ for temperature, $\text{mm}/10\text{a}$ for precipitation) of the seasonal and annual climatic components (T_{\min} , T_{\max} , T_{mean} , DTR, and precipitation) during 1958–2012 by the least square method

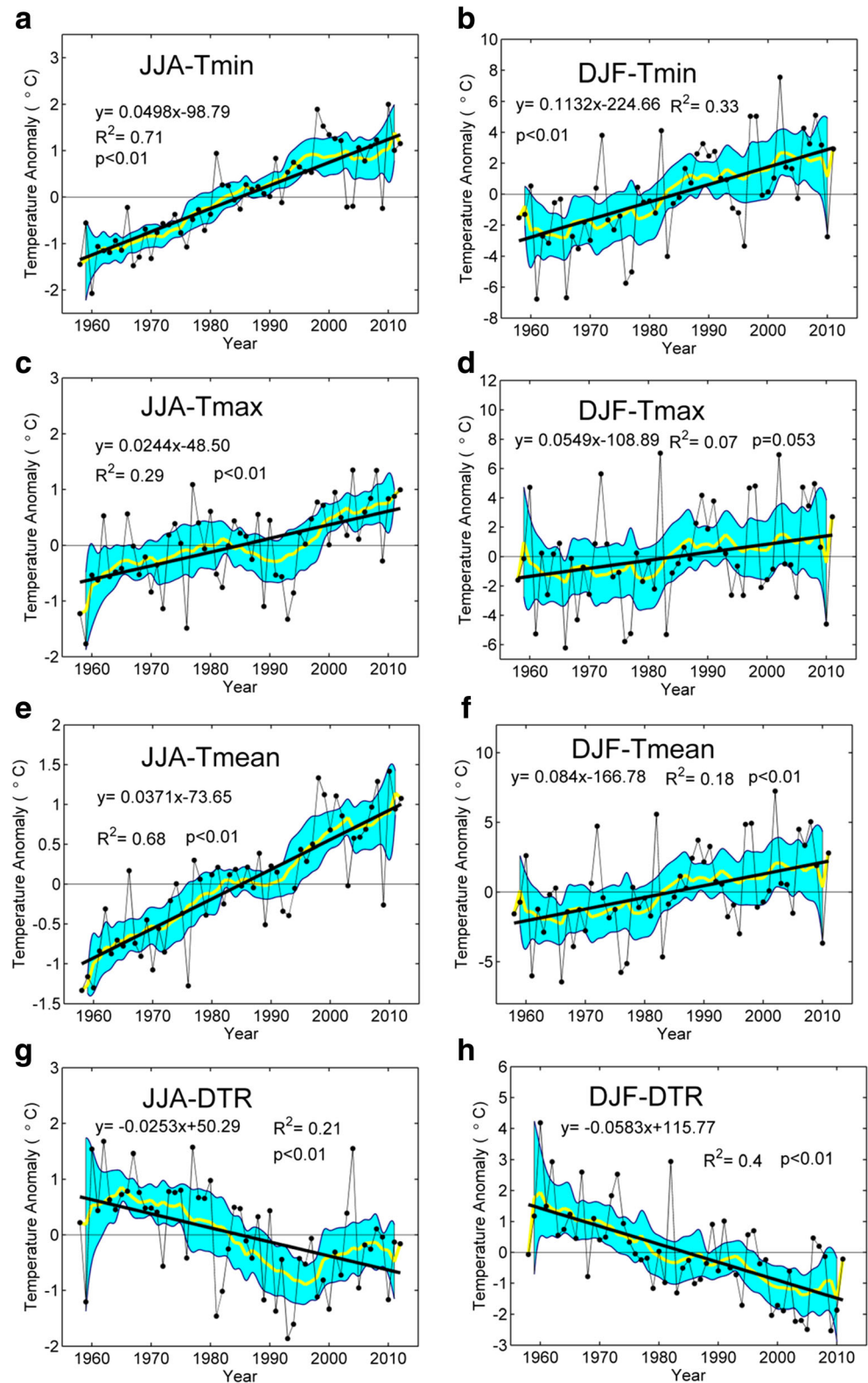
Time scale	T_{\min}	T_{\max}	T_{mean}	DTR	Precipitation
MAM	$0.44^{**} \pm 0.29$	$0.43^{**} \pm 0.39$	$0.43^{**} \pm 0.33$	-0.01	-1.18
JJA	$0.50^{**} \pm 0.11$	$0.24^{**} \pm 0.14$	$0.37^{**} \pm 0.09$	$-0.25^{**} \pm 0.18$	5.01
SON	$0.71^{**} \pm 0.31$	$0.48^{**} \pm 0.41$	$0.59^{**} \pm 0.33$	-0.24	1.88
DJF	$1.13^{**} \pm 0.60$	0.55	$0.84^{**} \pm 0.66$	$-0.58^{**} \pm 0.26$	$1.49^* \pm 1.19$
Annual	$0.67^{**} \pm 0.19$	$0.40^{**} \pm 0.25$	$0.54^{**} \pm 0.21$	$-0.27^{**} \pm 0.14$	7.17

*95 %, **99 % confidence interval

negative anomalies appear from 1958 to 1980 and after 1980, the positive anomalies appear (Fig. 2a). Compared with the annual T_{\min} trend, the trend of the annual T_{\max} and T_{mean} is $0.4 \text{ } ^\circ\text{C}/10\text{a}$ and $0.54 \text{ } ^\circ\text{C}/10\text{a}$, respectively. Further, annual

T_{\min} , T_{\max} , and T_{mean} have the same temporal variations (Fig. 2a–c). The bigger increasing trend of the T_{\min} than the T_{\max} consequently results in a significant decreasing trend ($p < 0.01$, $-0.27 \text{ } ^\circ\text{C}/10\text{a}$) of the DTR (Fig. 2d). This finding

Fig. 3 The temperature anomalies trends for JJA (left panel) and DJF (right panel) during 1958–2012. From top to bottom is for T_{\min} , T_{\max} , T_{mean} , and DTR, respectively. The legends are same as in Fig. 2



is in agreement with the previous studies (Liu et al. 2006; Su et al. 2006; Donat et al. 2013).

In the seasonal temperature changes, all the temperature indices show a significant increasing trend ($p < 0.01$) except the T_{\max} trend in DJF (see Table 2). Particularly, the biggest increasing trends appear in DJF for T_{\min} (1.13 ± 0.60 °C/10a), T_{\max} (0.55 °C/10a), and T_{mean} (0.84 ± 0.66 °C/10a), followed by the trends in SON. And the smallest increasing trends appear in MAM for T_{\min} and in JJA for T_{\max} and T_{mean} . The DTR has a significant decreasing trend at a 99 % confidence level only in JJA (-0.25 ± 0.18 °C/10a) and DJF (-0.58 ± 0.26 °C/10a). The nonsignificant decreasing trend (-0.01 °C/10a) of the DTR in MAM may be caused by the same variation pattern in T_{\min} and T_{\max} , and the slight difference of the increasing trend (Table 2) between them. Further, the bigger magnitude is found in DJF than in JJA for T_{\min} , T_{\max} , T_{mean} , and DTR which indicates a stronger change of the temperature in DJF than in JJA during 1958–2010 (Fig. 3).

For the precipitation, Fig. 4a shows that the annual precipitation anomaly has an increasing trend (7.17 mm/10a) in the period 1958–2012 although it is not significant at 90 % confidence level. In fact, the quadratic polynomial may fit the annual precipitation change better than the linear fit. Before the early 1980s, the annual precipitation has a sharp decrease, and then it becomes an increasing trend. This finding indicates the nonlinear characteristic of the precipitation in Bayanbuluk. In the seasonal precipitation changes, there exist increasing trends in JJA, SON, and DJF, except a decreasing trend

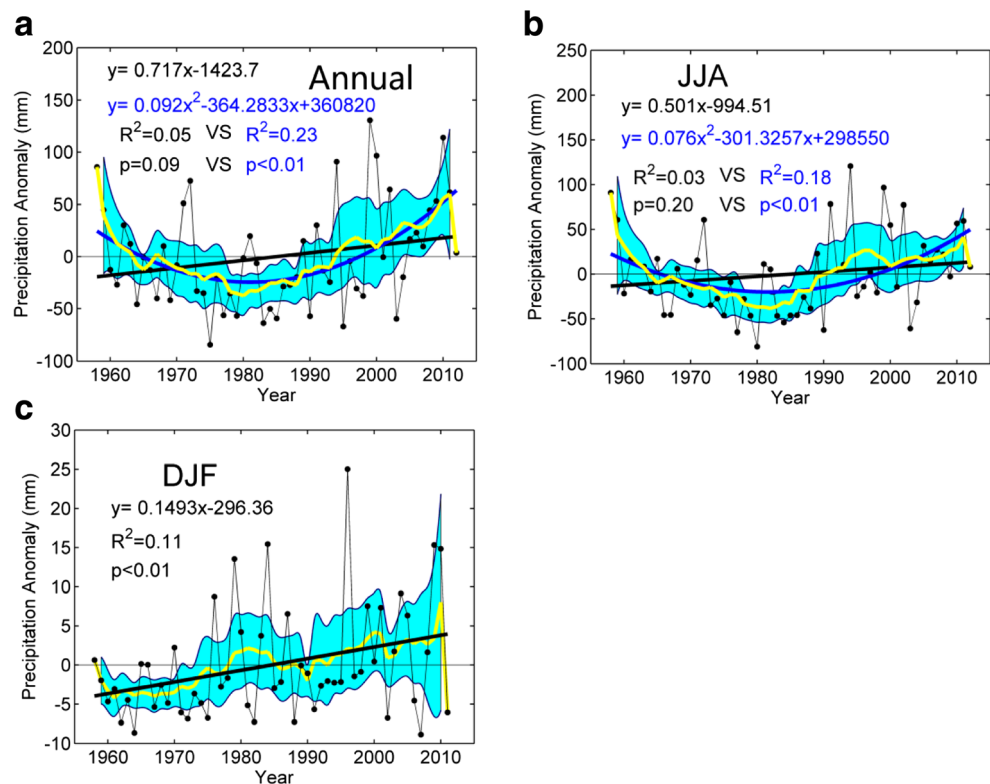
(-1.18 mm/10a) in spring during this period (Table 2). Comparing with the other three seasons, the summer precipitation has the biggest contribution to the annual total precipitation with an increasing trend (5.01 mm/10a) and a nonlinear change also appears annually in Fig. 4b. The increasing trend (1.49 ± 1.19 mm/10a) of the precipitation anomaly in winter is significant at the 95 % confidence level (Fig. 4c).

Figure 5 shows the averaged monthly precipitation during the period 1958–2012. It is found that July has the biggest precipitation than other months, and the average precipitation is 69 mm which is more than 23 times that of the smallest precipitation in January. Then, it is followed by the June and August precipitation. The precipitation in May is comparable to September. On the whole, the precipitation in warm season (May–September) accounts for the vast majority part (87 %) of precipitation in the year. The above results have a well explanation for the same temporal trend between the summer and annual precipitations.

3.2 The abrupt climate change and LRD

In this section, the Mann-Kendall method is used to detect the abrupt climate change and the Hurst index is used to investigate the LRD. Table 3 displays that the annual T_{\min} , T_{\max} , and T_{mean} have the same abrupt climate change at the middle of the 1980s, and the abrupt climate change year appears at 1984, 1987, and 1985, respectively. The annual DTR has an abrupt climate change year at 1978. After the climate abrupt change,

Fig. 4 The precipitation anomalies trend for annual (a), JJA (b), and DJF (c) during 1958–2012, respectively. The blue curve is the quadratic polynomial fit result which is significant at a 99 % confidence level. The other legend is same as in Figs. 2 and 3 but for precipitation anomalies



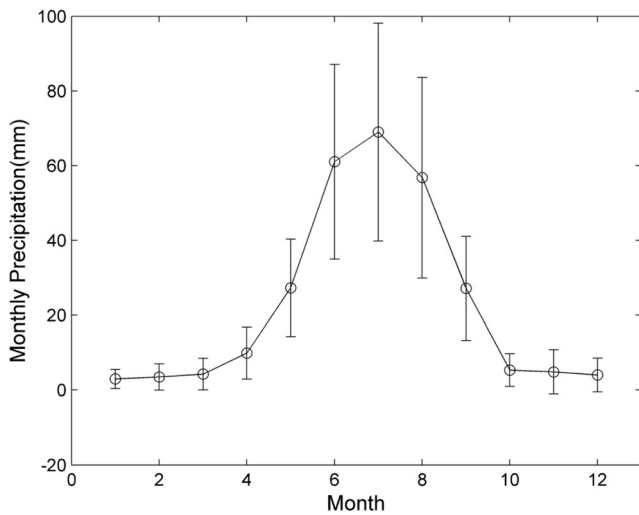


Fig. 5 Variation in averaged monthly precipitation during 1958–2012 in Bayanbuluk area. And the standard deviation is also added to provide the variation of the monthly values

the averaged increasing trend value is decreased for the annual T_{min} (decreased $0.1\text{ }^{\circ}\text{C}/10\text{a}$) and the annual T_{max} (decreased $0.01\text{ }^{\circ}\text{C}/10\text{a}$), and the increasing trend of the annual T_{mean} becomes bigger (increased $0.05\text{ }^{\circ}\text{C}/10\text{a}$). In the seasonal abrupt climate change, the temperature indices in SON have the same abrupt climate change year at 1987 which is consistent with the annual T_{max} . However, the DTR in SON has no significant abrupt climate change. In winter, the abrupt climate change year of the T_{min} and T_{mean} is at 1984 which is same with the annual T_{min} . But the abrupt climate change of the T_{max} is not significant. In other seasons, abrupt climate change of the temperature indices is different. For the precipitation, only abrupt climate change is found at winter and the abrupt year is 1992. The annual and the other three season precipitations have no significant abrupt climate change.

Figure 6 provides the Hurst index results for the T_{min} , T_{max} , T_{mean} , and precipitation at seasonal and annual scales during 1958–2012. The H values are bigger than 0.5 which indicates the long-term memory with the same trend in future for the

Table 3 Results of the abrupt climate changed by Mann-Kendall method

Time scale	Climate factor	Before abrupt			Abrupt year	After abrupt		
		K	Mean	Var		K	Mean	Var
MAM	T_{min}	0.35	-9.06	1.78	1992	0.32	-7.73	1.74
	T_{max}	0.25	5.42	2.79	1996	-0.14	7.01	3.44
	T_{mean}	0.33	-1.78	2.11	1995	0.09	-0.34	2.45
	DTR				NSA			
	Precipitation				NSA			
JJA	T_{min}	0.38	2.13	0.21	1980	0.31	3.69	0.40
	T_{max}	0.10	17.22	0.44	1996	0.18	18.14	0.21
	T_{mean}	0.44	9.73	0.26	1983	0.40	10.73	0.30
	DTR	0.06	15.04	0.47	1980	0.10	14.00	0.55
	Precipitation				NSA			
SON	T_{min}	0.72	-10.52	2.23	1987	0.64	-8.49	1.89
	T_{max}	0.45	5.12	3.00	1987	-0.08	6.67	3.13
	T_{mean}	0.59	-2.70	2.08	1987	0.28	-0.91	1.96
	DTR				NSA			
	Precipitation				NSA			
DJF	T_{min}	0.68	-32.02	7.08	1984	0.51	-28.45	6.22
	T_{max}				NSA			
	T_{mean}	0.29	-24.45	8.72	1984	0.28	-21.67	7.15
	DTR	-0.41	15.56	1.46	1976	-0.38	13.70	1.33
	Precipitation	14.4	8.74	33.26	1992	6.9	13.12	75.89
Annual	T_{min}	0.69	-12.23	0.87	1984	0.59	-10.32	1.00
	T_{max}	0.23	2.80	0.94	1987	0.22	4.10	1.48
	T_{mean}	0.41	-4.73	0.81	1985	0.46	-3.13	1.13
	DTR	-0.02	15.24	0.38	1978	-0.09	14.28	0.36
	Precipitation				NSA			

The K value ($^{\circ}\text{C}/10\text{a}$) is the change trend before or after the abrupt year computing by the linear least square method. Var is the variance and NSA is non-significant abrupt ($p > 0.05$)

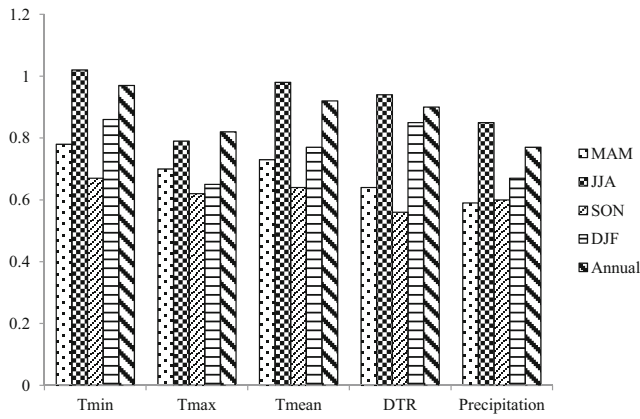


Fig. 6 The Hurst index of the seasonal and annual climatic components (T_{min} , T_{max} , T_{mean} , DTR, and precipitation) during 1958–2012

temperature and precipitation. For the annual temperature, the T_{min} has the biggest H value (0.97), followed by T_{mean} (0.92) and T_{max} (0.82). It shows that the temperature will have a sustained increasing trend and this trend of T_{min} is bigger than that of the T_{max} . The range of the temperature will be small because of the $H = 0.9 > 0.5$ for the annual DTR. For the precipitation, the Hurst index values are bigger than 0.5. The Hurst index of the spring precipitation is 0.59 which indicates a continuous decreasing trend in future. In summer, the precipitation has the biggest Hurst index value ($H = 0.85$) than the other seasons which suggests the strongest increasing tendency.

3.3 The extremes of the temperature and precipitation

The cold nights (TN10p) and cold days (TX10p) show significant ($p < 0.01$) decreasing trends, and the corresponding trend

Fig. 7 The trends of the cold nights (TN10p), warm nights (TN90p), cold days (TX10p), warm days (TX90p), and growing season length (GSL) during 1958–2012, respectively. All the trends are significant at a 99 % confidence level

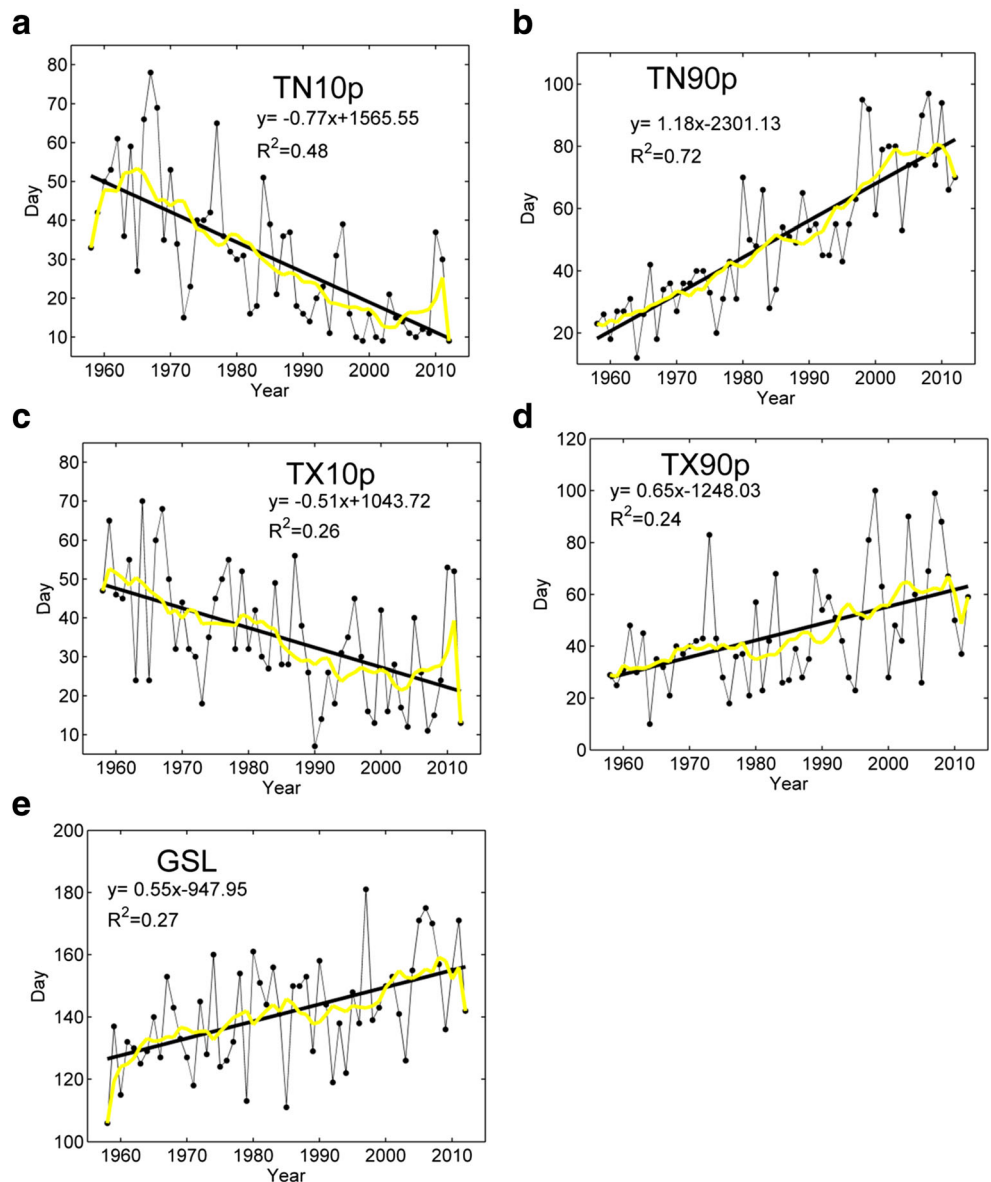


Fig. 8 The trends of the RX1day (maximum 1-day precipitation amount) (a), R10mm (number of heavy precipitation days) (b), CDD (consecutive dry days) (c), and R95pTOT (very wet days) (d), respectively. The red line and blue line are the linear fit results for different periods. The formulas with different colors are corresponding to the different colors linear fit lines computed by the least square method. The red linear fit line for 1958–1980 (a, d) and 1958–1983 (b). The blue linear fit line for 1981–2012 (a, d) and 1984–2012 (b). The black linear fit line is for the whole period 1958–2012

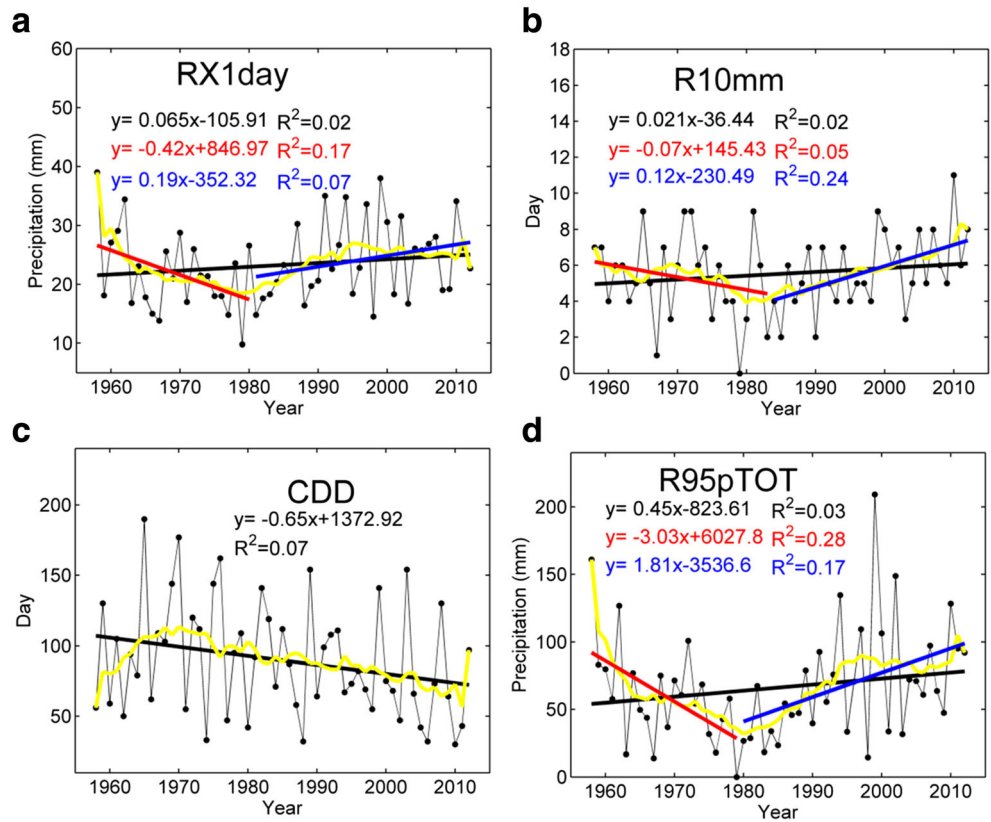
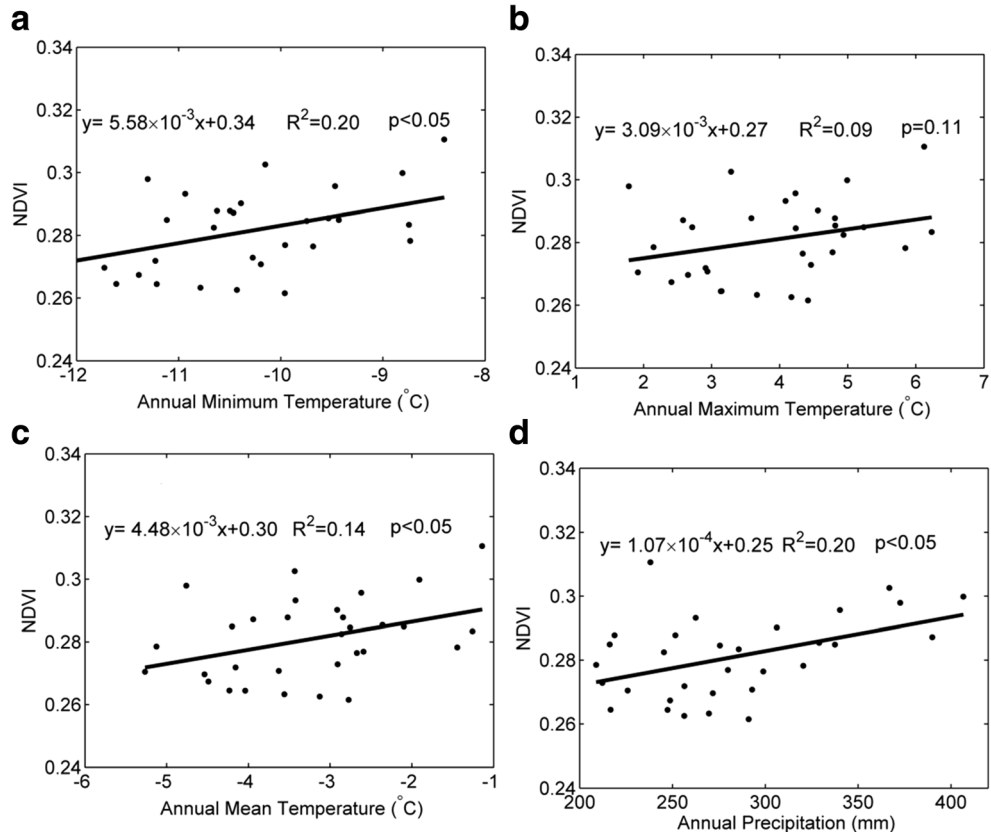


Fig. 9 The relationship between the annual NDVI and four climate factors: annual T_{min} (a), annual T_{max} (b), annual T_{mean} (c), and annual precipitation (d)



values are 7.7d/10a and 5.1d/10a (Fig. 7a, c). On the other hand, the warm nights (TN90p) and warm days (TX90p) have greatly linear increases at a 99 % confidence level with the increasing trend values 11.8d/10a and 6.5d/10a (Fig. 7b, d). The increasing in warm nights (or days) and the decreasing in cold nights (or days) directly prolong the growing season length (GSL) with a significant increasing trend (5.5d/10a) over Bayanbuluk grassland in 1958–2012.

Figure 8a–d displays the trends of the precipitation indices including the RX1day, R10mm, CDD, and R95pTOT, respectively. A slight increase (0.65 mm/10a) for the RX1day is found in Fig. 8a during 1958–2012. In fact, this trend is grouped by a significant decrease (−4.2 mm/10a, $p < 0.05$) in 1958–1980 and an increased trend (1.9 mm/10a) in 1981–2012. The frequency of the R10mm is decreased (−0.7d/10a) from 1958 to 1983, and then it has a significant increasing trend (1.2d/10a, $p < 0.05$) during 1984–2012 (Fig. 8b). The trend of the whole period 1958–2012 is 0.21d/10a. For the consecutive dry days (CDD) change, Fig. 8c shows a decreasing trend (−6.5d/10a). Lastly, the change of the R95pTOT (Fig. 8d) has a significant decreasing trend (−30.3 mm/10a,

$p < 0.05$) in 1958–1980 and a significant increasing trend (18.1 mm/10a, $p < 0.05$) from 1981 to 2012 which is similar with the changes of the RX1day and R10mm (Fig. 8a, b). In fact, it is clear that the variations of the RX1day, R10mm, and R95pTOT are same as that of the annual and JJA precipitation (Fig. 4a, b) which indicates that the RX1day, R10mm, and R95pTOT have a large contribution to the annual total precipitation, at least to the summer precipitation.

In order to compare with the abrupt change and the LRD of the averaged climate records, we further detect the climate extreme events by the Mann-Kendall method and Hurst index. The TN10P and TN90P have the same abrupt change at 1985 which is close to the abrupt change year of the annual T_{\min} (1984). However, the abrupt change year of the TX10P (1980) is different from that of the TX90P (1988). And the abrupt change year of the T_{\max} and T_{mean} is at 1987 and 1985, respectively. On the whole, it can be certain that the abrupt change of the temperature appears at the mid-to-late 1980s. From the piecewise fitting results of the extreme precipitation indices in Fig. 8a (RX1day), Fig. 8b (R10mm), and Fig. 8d (R95pTOT), we can directly obtain that there is a change of

Table 4 Comparison of decadal temperature (precipitation) change rate ($^{\circ}\text{C}/10\text{a}$ and $\text{mm}/10\text{a}$) in Bayanbuluk grassland from 1958 to 2012 derived from this study to rates reported in other studies

Studies	Study area	Study period	Data and methods	Annual	MAM	JJA	SON	DJF
Aizen 1997	Tian Shan mountain	1940–1991	Observations from 110 stations	0.10				
Yin et al. 2015	Tian Shan mountain	1958–2001	NCEP-RegCM	0.12 (−8.6)				
			ERA40-RegCM	−0.01 (3)				
			CRU	0.30 (−3.1)				
			WM	0.23 (−1.1)				
Xu et al. 2015	Northern Xinjiang	1960–2011	Observations from 22 stations	0.35 (11.2)				
Li et al. 2011	Xinjiang	1961–2005	Observations from 65 stations	0.28 (4.12)	0.12 (−1.08)	0.12 (1.8)		0.45 (2.1)
Li and Wang 2012	northwest China	1960–2010	Observations from 74 stations	0.34				
Ren et al. 2005	China	1951–2004	Observations from 740 stations	0.25		0.15		0.39
Yao and Chen 2015	Syr	1881–2011	Observations from 8 stations	0.14 (4.44)				
Hu et al. 2014	CAS and Xinjiang	1979–2011	Observations from 81 stations	0.41	0.64	0.38	0.52	−0.01
			CRU	0.42	0.81	0.25	0.46	0.16
			CFSR	0.36	0.74	0.22	0.42	0.02
			ERA-Interim	0.36	0.69	0.24	0.49	0.05
			MERRA	0.36	0.75	0.36	0.47	−0.28
			CRU	0.33	0.34	0.23	0.32	0.47
	1960–2009	CRU	0.33	0.34	0.23	0.32	0.47	
	1960–2011	Observations from 62 stations	0.27	0.23	0.19	0.31	0.33	
Our Study	Bayanbuluk	1958–2012	Observations from the Bayanbuluk station	0.54 (7.17)	0.43 (−1.18)	0.37 (5.01)	0.59 (1.88)	0.84 (1.49)

The numbers inside the pairs of parentheses in each column are the precipitation change rates.

CAS Central Asia States, OBS observations, GCMs general circulation models, CRU climate research unit (<http://www.cru.uea.ac.uk/cru/data/temperature>), NCDC National Climatic Data Center, USA

the climate state which is from the decreasing trend to the increasing trend after the early 1980s. The above results show that this climate transformation over the Bayanbuluk grassland is similar with the Xinjiang (Zhang et al. 2012) and the northwest of China (Shi et al. 2007). In addition, we should note that after the early 1980s, the increasing trend of the heavy precipitation extremes may lead to the increased risk of the floods over this area. According to the H values, the 9 climate extremes indices all have long-term memory characteristics. The decreasing trends for the TN10p ($H = 0.99$) and TX10p ($H = 0.86$) may continue into the future, and the increasing trends TN90p ($H = 0.93$) and TX90p ($H = 0.73$) may also be persistent. Although there are slight increasing trends for RX1day, R10mm, and R95pTOT during 1958–2012, their increasing trends may be continuous in the future ($H = 0.86$, 0.81 and 0.87, respectively).

There is a general agreement that the vegetation change can be recognized as an indicator of climate change (Piao et al. 2006; Shi et al. 2007; Hoover et al. 2014). For detecting the effects of climate change on vegetation over this area, we detect the relationships between the normalized difference vegetation index (NDVI) and the annual T_{\min} , annual T_{\max} , annual T_{mean} , and annual precipitation. The NDVI data with a spatial resolution of $8 \times 8 \text{ km}^2$ and 15-day interval are downloaded from the Global Inventory Monitoring and Modeling Studies (GIMMS) group derived from the advanced very high-resolution radiometer (AVHRR) of the National Oceanic and Atmospheric Administration (NOAA) Land data set for the period January 1982 to December 2012 (<ftp://ftp.glcg.umiacs.umd.edu/glcg/GIMMS/>, Tucker et al. 2005). The annual NDVI is significantly ($p < 0.05$) positively correlated with the annual T_{\min} ($R^2 = 0.2$), annual T_{mean} ($R^2 = 0.14$), and annual precipitation ($R^2 = 0.20$) except the little correlation with the annual T_{\max} ($R^2 = 0.09$) (Fig. 9). This result indicates that the vegetation NDVI in Bayanbuluk grassland is mainly controlled by the minimum temperature and precipitation. The increased precipitation and T_{\min} provide favorable water-heat condition to improve the vegetation over this grassland from 1982 to 2012.

4 Discussion

Our results show a significant increasing trend ($0.54 \text{ }^\circ\text{C}/10\text{a}$) for the

annual T_{mean} in Bayanbuluk grassland during the period 1958–2012. This change rate is larger than the rate averaged for Central Asia (i.e., $0.39 \text{ }^\circ\text{C}/10\text{a}$ from 1979 to 2011) (Table 4, Hu et al. 2014), and it is also larger than the northwest of China ($0.34 \text{ }^\circ\text{C}/10\text{a}$ from 1960 to 2010, Li et al. 2012). This rate is about twice as large as the warming rate in Xinjiang ($0.28 \text{ }^\circ\text{C}/10\text{a}$ from 1961 to 2005, Li et al. 2011) and bigger than the two times of warming rate in China

($0.25 \text{ }^\circ\text{C}/10\text{a}$ from 1951 to 2004, Ren et al. 2005). It has been reported that temperature increase in many regions around the world has occurred most prominently in the winter months. Winter warming contributed strongly to the annual temperature increase (Huang et al. 2005; Ren et al. 2005; Li et al. 2011). Our seasonal results are consistent with this conclusion.

For the precipitation change, the Bayanbuluk grassland experienced a wetting trend ($7.17 \text{ mm}/10\text{a}$) during 1958–2012. This increasing trend of the precipitation is also found in north Xinjiang ($11.2 \text{ mm}/10\text{a}$, Xu et al. 2015) during 1960–2011, Xinjiang ($4.12 \text{ mm}/10\text{a}$, Li et al. 2011) during 1961–2005, and northwest of China (Wang et al. 2013). The RX1day, R10mm, and R95pTOT show increased trends, especially after the early 1980s. This suggests that the precipitation increase in Bayanbuluk grassland is due to the increase in both precipitation frequency and intensity. On the other hand, it indicates that the increased extreme precipitation will cause the increasing of the flood risks in this area, and this will happen in Tianshan Mountain and Xinjiang (Zhang et al. 2012).

As a consequence of global warming and an enhanced water cycle, the climate transformation (from a warm-dry to a warm-wet) in Bayanbuluk grassland appears at the 1980s (the abrupt change in 1985 for the annual T_{mean} and in 1987 for the SON temperature, the abrupt change in the early 1980 for the precipitation) which is similar to those found in northern Xinjiang (Xu et al. 2015, the abrupt change in 1986 for temperature and in 1987 for precipitation), Xinjiang, and northwest China (Shi et al. 2007; Li et al. 2011; Wang et al. 2013). In addition, our results show that all the records (averaged and extreme climate) are characterized by the LRD, and this is also found in Xinjiang (Li et al. 2011). It is suggested that the warm-wet tendency will be continuous into the future in this area. Further, the increased magnitude and frequency of the extreme climate events may affect the fragile grassland ecosystem which we have to face in the future.

Some valuable climate information is provided for computing the grassland area, grassland productivity, and helping water resource management in this area. However, the relationships between the climate change and the grassland ecosystem (such as the grassland productivity, vegetation coverage, vegetation type, and local carbon cycle) are not detected in this study. The previous studies (Sillmann et al. 2013a; Hu et al. 2014) suggest that the climate models or some climate datasets with high spatial resolutions may be an efficient way to describe the spatial climate change, especially in mountain areas (Yin et al. 2015), and the climate models also can project the future climate (Sillmann et al. 2013b). It will be interesting to detect the spatial pattern of the climate change by the climate models or some climate datasets with high spatial resolutions in this region with complex topography. These topics will leave for our future study.

5 Conclusions

This study analyzed the climate variations in the temperature and precipitation extreme events in Bayanbuluk grassland of Central Asia during 1958–2012. The major conclusions are summarized as follows:

- (a) The annual temperature has a significant increasing trend ($p < 0.01$) and the greatest warming is found for the annual T_{\min} (0.67 °C/10a). The bigger increasing trend of the annual T_{\min} than the T_{\max} induced a significant decreasing trend (−0.27 °C/10a) for the annual DTR. The seasonal temperature (including T_{\min} , T_{\max} , and T_{mean}) shows significant increasing trends ($p < 0.01$) except the nonsignificant increasing trend (0.55 °C/10a) for the T_{\max} in winter. The winter (DJF) temperature has the largest contribution to the warming of the annual temperature than the other three seasons.
- (b) The annual precipitation has a linear increasing trend (7.17 mm/10a) in Bayanbuluk grassland during 1958–2012. In fact, the annual total precipitation exhibits more nonlinear characteristics than the linear trend (Fig. 4a). The precipitation in JJA, SON, and DJF shows an increasing trend except the decreasing in MAM. Further, the wetting trend DJF is significant at a 99 % confidence level. The precipitation in JJA has the same nonlinear temporal characters as the precipitation which indicates that the precipitation across the Bayanbuluk grassland falls mainly in JJA.
- (c) There are significant warming trends for TN90p, TX90p, TN10p, and TX10p. The frequency and intensity of the precipitation extreme events are increasing. The R95pTOT mainly contributes to the annual precipitation with a linear trend 4.5 mm/10a. RX1day, R95pTOT, and R10mm all appear a sharp decreasing trend before the early 1980s, and after that time, they become increasing.
- (d) The temperature experienced the abrupt change at the mid-1980s. For the precipitation, there is a wetting transform at the early 1980s. The climate in the Bayanbuluk grassland has the LRD characteristic which means that the warm-wet tendency may be continuous into the future in this area.

Acknowledgments The authors are very grateful to the editor and anonymous referees for their valuable comments and helpful suggestions, which led to a great improvement of the original manuscript. This study was supported by the National Science Foundation of China (Project 11401569), the International Cooperation and Exchanges of the National Science Foundation of China (Project 41361140361), the Natural Science Foundation of Xinjiang (2014211B047), the Ministry of Science and Technology of China (No. GYHY201406016), and the National Science Foundation of China (Project 41301039, 41461023).

References

- Aizen VB coauthors (1997) Climatic and hydrologic changes in the Tien Shan, central Asia. *J Clim* 10:1393–1404
- Alexander L, Zhang X, Peterson T, et al (2006) Global observed changes in daily climate extremes of temperature and precipitation. *J Geophys Res* 111:D05109
- Alley R, Marotzke J, Nordhaus W, et al (2003) Abrupt climate change. *Science* 229:2005–2010
- Burn D, Mohamed A, Elnur H (2002) Detection of hydrologic trends and variability. *J Hydrol* 255:107–122
- Bloomfield P, Nychka D (1992) Climate spectra and detecting climate change. *Clim Chang* 21:275–287
- Changnon SA, Pielke J, Changnon D, et al (2000) Human factors explain the increased losses from weather and climate extremes. *Bull Am Meteorol Soc* 81:437–442
- Chen H, Sun J, Chen X (2014) Projection and uncertainty analysis of global precipitation-related extremes using CMIP5 models. *Int J Climatol* 34:2730–2748
- Chen X, Li B, Li Q, et al (2012) Spatio-temporal pattern and changes of evapotranspiration in arid Central Asia and Xinjiang of China. *J Arid Land* 4:105–112
- Dai L, Feng Y, Luo G, et al. (2015) The relationship between soil, climate and forest development in the mid-mountain zone of the Sangong River watershed in the northern Tianshan Mountains, China. *J Arid Land* 7:63–72
- Donat M, Alexander L, Yang H, et al. (2013) Updated analyses of temperature and precipitation extreme indices since the beginning of the twentieth century: the HadEX2 dataset. *J Geophys Res: Atmos* 118:1–16
- Easterling D, Horton B, Jones P, et al. (1997) Maximum and minimum temperature trends for the globe. *Science* 277:364–367
- Easterling D, Meehl G, Parmesan C, et al. (2000a) Climate extremes: observations, modeling, and impacts. *Science* 289:2068–2074
- Easterling D, Evans JL, Groisman P, et al. (2000b) Observed variability and trends in extreme climate events: a brief review. *Bull Am Meteorol Soc* 81:417–425
- Fraedrich K, Jiang J, Gerstengarbe F, et al (1997) Multiscale detection of abrupt climate changes: application to River Nile flood levels. *Int J Climatol* 17:1301–1315
- Frich P, Alexander L, Della-Marta P, et al. (2002) Observed coherent changes in climatic extremes during the second half of the twentieth century. *Clim Res* 19:193–212
- Hoover D, Knapp A, Smith M (2014) Resistance and resilience of a grassland ecosystem to climate extremes. *Ecology* 9:2646–2656
- Hu RJ et al. (2004) Physical geography of the TianShan Mountainous in China. China Environmental Sciences press, Beijing, pp. 140–141
- Hu Z, Zhang C, Hu Q, et al. (2014) Temperature changes in Central Asia from 1979 to 2011 based on multiple datasets. *J Clim* 27:1143–1167
- Hu Z, Zhang C, Luo G, et al (2013) Characterizing cross-scale chaotic behaviors of the runoff time series in an inland river of Central Asia. *Quat Int* 311:132–139
- Hurst HE (1951) The long-term storage capacity of reservoirs. *Trans Am Soc Civ Eng* 116
- Intergovernmental Panel on Climate Change (IPCC) (1995) In: Houghton JT et al. (eds) The science of climate change. Cambridge Univ. Press, Cambridge
- Intergovernmental Panel on Climate Change (IPCC) (2012) Managing the risks of extreme events and disasters to advance climate change adaptation. In: Field CB, Barros V, Stocker TF, et al. (eds) A special report of working groups I and II of the intergovernmental panel on climate change. Cambridge University Press, Cambridge
- Intergovernmental Panel on Climate Change (IPCC) (2013) In: Stocker TF, Qin D, Plattner G-K, Tignor M, Allen SK, Boschung J, Nauels A, Xia Y, Bex V, Midgley PM (eds) Climate change 2013: the

- physical science basis. Contribution of working group I to the fifth assessment report of the intergovernmental panel on climate change. Cambridge University Press, Cambridge 1535 pp
- Janowiak J (1990) The global climate of December 1989–February 1990: extreme temperature variations in north america, persistent warmth in Europe and Asia, and the return of ENSO-like conditions in the Western Pacific. *J Clim* 3:685–709
- Karl TR, Jones PD, Knight RW, et al. (1993) A new perspective on recent global warming: asymmetric trends of daily maximum and minimum temperature. *Bull Am Meteorol Soc* 74:1007–1023
- Karl TR, Nicholls N, Ghazi A (1999) CLIVAR/GCOS/WMO workshop on indices and indicators for climate extremes: workshop summary. *Clim Chang* 42:3–7
- Katz R, Brown B (1992) Extreme events in a changing climate: variability is more important than averages. *Clim Chang* 21:289–302
- Kendall MG (1948) Rank correlation methods. Hafner, 160 pp
- Kharin V, Zwiers F, Zhang X, et al. (2007) Changes in temperature and precipitation extremes in the IPCC ensemble of global coupled model simulations. *J Clim* 20:1419–1444
- Koutsoyiannis D (2003) Climate change, the Hurst phenomenon, and hydrological statistics. *Hydrol Sci-J Sci Hydrol* 48:3–24
- Koutsoyiannis D, Montanari A (2007) Statistical analysis of hydroclimatic time series: uncertainty and insights. *Water Resour Res* 43:W05429
- Li BF, Chen YN, Shi X (2012) Why does the temperature rise faster in the arid region of northwest China? *J Geophys Res* 117:D16115
- Li Q, Chen YN, Shen Y (2011) Spatial and temporal trends of climate change in Xinjiang, China. *J Geogr Sci* 21:1007–1018
- Li Q, Wang Y (2012) Changes in the observed trends in extreme temperatures over China around 1990. *J Clim* 25:5208–5222
- Liu X, Yin Z, Shao X, et al. (2006) Temporal trends and variability of daily maximum and minimum, extreme temperature events, and growing season length over the eastern and central Tibetan Plateau during 1961–2003. *J Geophys Res* 111:D19109
- Mann HB (1945) Nonparametric tests against trend. *Econometrica* 13: 245–259
- Mann M (2011) On long range dependence in global surface temperature series. *Clim Chang* 107:267–276
- McMichael A, Woodruff R, Hales S (2006) Climate change and human health: present and future risks. *Lancet* 367:859–869
- Patz J, Campbell-Lendrum D, Holloway T, et al (2005) Impact of regional climate change on human health. *Nature* 438:310–317
- Pei L, Moore N, Zhong S, et al. (2014) WRF model sensitivity to land surface model and cumulus parameterization under short-term climate extremes over the southern great plains of the United States. *J Clim* 27:7703–7724
- Peterson TC, and Coauthors (2001) Report on the activities of the working group on climate change detection and related rapporteurs 1998–2001. WMO, Rep. WCDMP-47, WMO-TD 1071, Geneva, Switzerland, 143pp
- Piao S, Mohammat A, Fang J, et al (2006) NDVI-based increase in growth of temperature grasslands and its response to climate changes in China. *Glob Environ Chang* 16:340–348
- Rea W, Reale M, Brown J (2011) Long memory in temperature reconstructions. *Clim Chang* 107:247–265
- Rehman S (2009) Study of Saudi Arabian climatic conditions using Hurst exponent and climatic predictability index. *Chaos, Solitons Fractals* 39:499–509
- Rehman S, Siddiqi AH (2009) Wavelet based Hurst exponent and fractal dimensional analysis of Saudi climatic dynamics. *Chaos, Solitons Fractals* 40:1081–1090
- Ren GY, Xu MZ, Chu ZY, et al. (2005) Changes of surface air temperature in China during 1951–2004. *Clim Environ Res* 10:717–727
- Rybski D, Bunde A, Havlin S, et al. (2006) Long-term persistence in climate and the detection problem. *Geophys Res Lett* 33:L06718
- Samorodnitsky G (2006) Long range dependence. *Found Trends Stoch Syst* 1:163–257
- Sanchez M, Trinidad SJ, Garcia PJ (2008) Some comments on Hurst exponent and the long memory processes on capital markets. *Phys A* 387:5543–5551
- Sakalauskiene G (2003) The Hurst phenomenon in hydrology. *Environ Res Eng Manag* 3:16–20
- Sayemuzzaman M, Jha M, Mekonnen A (2015) Spatio-temporal long term (1950–2009) temperature trend analysis in North Carolina, United States. *Theor Appl Climatol* 120:159–171
- Shi Y, Shen Y, Kang E, et al. (2007) Recent and future climate change in northwest China. *Clim Chang* 80:379–393
- Sillmann J, Kharin V, Zwiers F (2013a) Climate extremes indices in the CMIP5 multimodel ensemble: part 1. Model evaluation in the present climate. *J Geophys Res Atmos* 118:1716–1733
- Sillmann J, Kharin V, Zwiers F (2013b) Climate extremes indices in the CMIP5 multimodel ensemble: part 2. Future climate projections. *J Geophys Res Atmos* 118:2473–2493
- Su B, Jiang T, Jin W (2006) Recent trends in observed temperature and precipitation extremes in the Yangtze river basin, China. *Theor Appl Climatol* 83:139–151
- Sun Y, Zhang X, Zwiers F, et al. (2014) Rapid increase in the risk of extreme summer heat in eastern China. *Nat Clim Chang*. doi:10.1038/NCLIMATE2410
- The Ministry of Water Resources of the People's Republic of China, (1999) The great flood over China in 1998, China Water Conservancy Press, ISBN 7-5084-0037-2
- Thornton PK, Ericksen P, Herrero M, et al. (2014) Climate variability and vulnerability to climate change: a review. *Glob Chang Biol* 20: 3313–3328
- Tucker CJ, Pinzon JE, Brown ME, et al (2005) An extended AVHRR 8-km NDVI data set compatible with MODIS and SPOT vegetation NDVI data. *Int J Remote Sens* 26:4485–5598
- Velasquez Valle MA, Medina Garcia G, Cohen I (2013) Spatial variability of the Hurst exponent for the daily scale rainfall series in the state of Zacatecas, Mexico. *J Appl Meteorol Climatol* 52:2771–2780
- Wang H, Chen Y, Chen Z (2013) Spatial distribution and temporal trends of mean precipitation and extremes in the arid region, northwest of China, during 1960–2010. *Hydrol Process* 27:1807–1818
- Xu C, Li J, Zhao J, et al (2015) Climate variations in northern Xinjiang of China over the past 50 years under global warming. *Quat Int* 358: 83–92
- Xu W, Li Q, Wang X, Yang S, Cao L, Feng Y (2013) Homogenization of Chinese daily surface air temperatures and analysis of trends in the extreme temperature indices. *J Geophys Res Atmos* 118:9708–9720
- Yin G, Chen X, Tiyip T, et al. (2015) A comparison study between site-extrapolation-based and regional climate model-simulated climate datasets. *Geogr Res* 4:631–643
- Yao J, Chen Y. (2015) Trend analysis of temperature and precipitation in the Syr Darya Basin in Central Asia. *Theor Appl Climatol* 120:521–531
- Zhai P, Zhang X, Wan H, et al. (2005) Trends in total precipitation and frequency of daily precipitation extremes over China. *J Clim* 18: 1096–1108
- Zhang C, Li C, Chen X, et al. (2013) A spatial-explicit dynamic vegetation model that couples carbon, water, and nitrogen processes for arid and semi-arid ecosystems. *J Arid Land* 5:102–117
- Zhang Q, Singh V, Li J, et al. (2012) Spatio-temporal variations of precipitation extremes in Xinjiang, China. *J Hydrol* 434:7–18
- Zhang X, Hegerl G, Zwiers F, et al. (2005) Avoiding inhomogeneity in percentile-based indices of temperature extremes. *J Clim* 18:1641–1651
- Zhu X, Fraedrich K, Liu Z, et al. (2010) A demonstration of long-term memory and climate predictability. *J Clim* 23:5021–5029